



Preparation and characterization of single crystals of tetrakis(4-(5,5-dimethyl-2-phenyl-1,3-dioxan-2-yl)phenyl)germane

Tae Won Lee^a, Dong Woo Lee^b, Yeonjeong Choi^a, Kang Min Ok^{b,*}, Kwangyong Park^{a,*}

^a School of Chemical Engineering and Materials Science, Chung-Ang University, Seoul, 06974, Republic of Korea

^b Department of Chemistry, Chung-Ang University, Seoul, 06974, Republic of Korea



ARTICLE INFO

Article history:

Received 13 July 2018

Accepted 17 September 2018

Available online 9 October 2018

Keywords:

Organogermanium compound

Single crystal

Tetrahedral

Gas adsorption

Second-harmonic generating efficiency

ABSTRACT

A novel tetrakis(4-(5,5-dimethyl-2-phenyl-1,3-dioxan-2-yl)phenyl)germane (**2**) was synthesized by the reaction of germanium(IV) tetrachloride with 4-(5,5-dimethyl-2-phenyl-1,3-dioxan-2-yl)phenyllithium. Colorless plate-shaped single crystals obtained from recrystallization in ether were characterized by the single-crystal X-ray diffraction. The organogermanium compound was crystallized in a noncentrosymmetric nonpolar tetragonal space group, *I*-4, and classified as a porous molecular material owing to the presence of two types of distinct channels as a result of intermolecular hydrogen bonding. Compound **2** exhibits a differential gas adsorption property. The powder second-harmonic generating (SHG) measurements indicate that compound **2** shows a SHG efficiency 10 times greater than those of α -SiO₂ and type-1 nonphase-matchable.

© 2018 The Korean Society of Industrial and Engineering Chemistry. Published by Elsevier B.V. All rights reserved.

Compounds with a molecular structure enhancing an intermolecular π - π overlap are generally known to possess good charge-transporting properties [1]. However, such intermolecular π - π overlap of planar π -conjugated compounds easily leads to π - π stacking that tends to cause serious problems such as electric shortage by partial crystallization and nonradiative recombination by forming aggregates in the devices [2–4]. Efforts to reduce the π - π stacking by transforming the molecular structure to three dimension, such as tetrahedral, dendric, and spiro, have been reported previously [5–10]. We also reported several tin-cored tetrahedral stilbene compounds and applied in OLEDs [11].

As a part of our ongoing investigation for developing tetrahedral optoelectronic materials, a germanium-cored benzophenone intermediate was required to construct tetrahedral stilbene or distyrylarylene germanium compounds. 2-(4-Bromophenyl)-5,5-dimethyl-2-phenyl-1,3-dioxane (**1**), a protected analogue of benzophenone, was initially prepared by the reaction of 4-bromobenzophenone with 2,2-dimethyl-1,3-propanediol. The reaction of germanium(IV) chloride (GeCl₄) with 4-(5,5-dimethyl-2-phenyl-1,3-dioxan-2-yl)phenyllithium, pre-prepared *in situ* by the reaction of **1** with *n*-BuLi, produced tetrakis(4-(5,5-

dimethyl-2-phenyl-1,3-dioxan-2-yl)phenyl)germane (**2**) as a single crystal in a good yield after recrystallization from ether.

Herein, we report our efforts toward the synthesis and crystallization, crystal structure determination, and characterization of a novel noncentrosymmetric (NCS) tetrahedral compound **2**. Materials crystallizing with macroscopic NCS structures may exhibit interesting frequency conversion properties. In addition, the structure of the title compound reveals a porosity attributable to the intermolecular hydrogen bonding interactions. Second-order nonlinear optical (NLO) properties and a selective gas adsorption phenomenon for **2** are also presented.

Intermediate compound **1** was prepared by the reaction of 4-bromobenzophenone with 2,2-dimethylpropane-1,3-diol. The crude product was recrystallized from *iso*-propanol, affording pale pink plate-shaped crystals in 83% isolated yield. Tetrahedral germanium compound **2** was prepared by the reaction of GeCl₄ with four equivalents of 4-(5,5-dimethyl-2-phenyl-1,3-dioxan-2-yl)phenyllithium, prepared by the reaction of **1** with *n*-BuLi *in situ* (Fig. 1). The crude product was recrystallized from ether, affording colorless plate-shaped single crystals in 83% isolated yield.

Abbreviations: SHG, Second-harmonic generating; OLED, Organic light-emitting diode; CCD, Charge-coupled device; XRD, X-ray diffraction; PXRD, Powder XRD; TGA, Thermogravimetric analysis; NLO, Second-order nonlinear optical; ADP, NH₄H₂PO₄; ESI, Electronic supplementary information; NCS, Noncentrosymmetric; MP, Melting points; TMS, Tetramethylsilane.

* Corresponding authors.

E-mail addresses: kmok@cau.ac.kr (K.M. Ok), kypark@cau.ac.kr (K. Park).

<https://doi.org/10.1016/j.jiec.2018.09.024>

1226-086X/© 2018 The Korean Society of Industrial and Engineering Chemistry. Published by Elsevier B.V. All rights reserved.

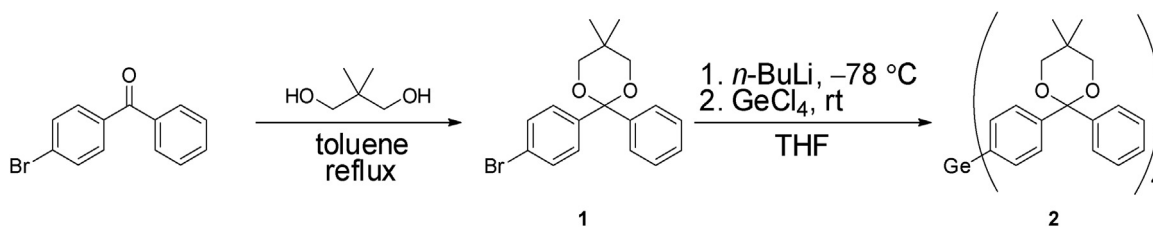


Fig. 1. Synthesis of compound 1.

Compound **2** is a molecular material crystallizing into a NCS tetragonal space group, *I*-4 (No. 82). Four 4-phenyl-5,5-dimethyl-2-phenyl-1,3-dioxane ligands are connected to Ge^{4+} cation through covalent C—Ge bonds (Fig. 2a). The unique Ge^{4+} cation is in a four-coordinate tetrahedral coordination environment with the Ge—C bond distances of 1.940(3) Å. The observed C(1)—Ge(1)—C(1) bond angles are 105.8(2)° and 111.36(12)°. The C—O and C—C bond distances in the ligand are in the range 1.404(4)–1.445(4) Å and 1.344(10)–1.548(5) Å, respectively. The selected bond distances are listed in Table 2. Interestingly, intermolecular hydrogen bonding occurs between the O(2) in the dioxane moiety in one ligand and the C(12) in the phenyl group in the adjacent ligand [O(2) . . . C(12) 3.422(9) Å], resulting in both square-like and rectangular channels along the [001] direction (Fig. 2b). While the dimensions of the square-like channels are approximately 5.8 Å × 5.8 Å, those of the rectangular channels are approximately 4.0 Å × 11.1 Å in the framework. Thus, the framework of compound **2** can be considered as a pseudo-three-dimensional structure with unprecedented channels. In other words, the compound can be considered as a molecular porous material attributed to the channel structure originating from the intermolecular hydrogen bonding. The CALC SOLV command in the PLATON crystallographic program suggests that compound **2** contains ~ 6% of empty space [12]. The crystallographic data can be found in the ESI.

The thermal behavior of compound **2** was investigated by thermogravimetric analysis. The compound is thermally stable up to 320 °C, as indicated by the thermogravimetric analysis diagram (see the ESI). At temperature > 320 °C, however, decomposition

occurs because of the loss of organic ligands. The thermal stability of compound **2** was also confirmed by the powder XRD (PXRD) pattern. No substantial changes in the peak position and intensity were observed in the PXRD data measured up to 300 °C. However, the PXRD pattern obtained at 500 °C reveals decomposed amorphous phases. The TGA diagram and PXRD data measured at different temperatures can be found in the ESI.

Since compound **2** reveals a channel structure attributed to the intermolecular hydrogen bonding, adsorption experiments with a few different gases were performed. Initially, compound **2** was evacuated at 100 °C for 3 h to remove any moisture or solvent inside the channels. The N_2 and H_2 did not diffuse significantly into the channels at 77 K (Fig. 3a). However, interestingly, as shown in Fig. 3a, the adsorption capacity of compound **2** for CO_2 at 195 K is significantly greater. Similar differential gas adsorptions in frameworks containing channels have been reported previously [13–18]. The low hydrogen adsorption for compound **2** may be attributed to the lack of appropriate sites of metal ions and ligands that can strongly interact with H_2 molecules. Meanwhile, the substantial quadruple interactions of N_2 with the electrostatic field gradients near the surface may strongly interact with the N_2 molecules with the pore windows, thus subsequently obstructing other molecules from passing into the channel [19]. With the CO_2 at 195 K, however, such interactions overcome by thermal energy. Further analyses of the experimental data estimated by the Langmuir surface area and the SF method yields the surface area of 105 m^2/g based on CO_2 adsorption and approximate pore diameters in the range 8–12 Å, respectively. The measured channel size of compound **2** is

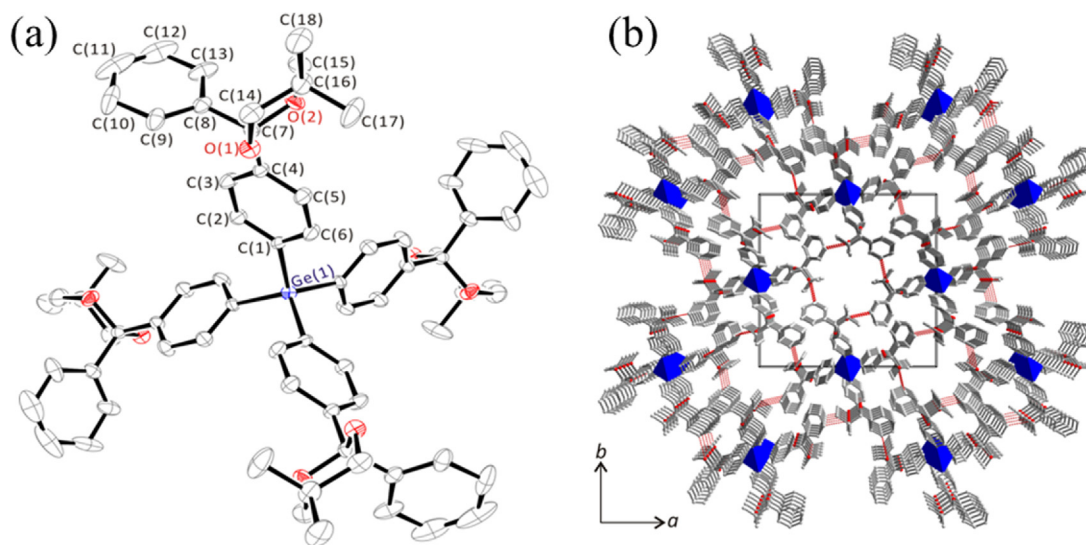


Fig. 2. (a) ORPEP (30% probability ellipsoids) drawing representing the coordination environment of compound **2**. Hydrogen atoms were removed for clarity. (b) Ball-and-stick and polyhedral diagram showing a channel structure of compound **2** in the *ab*-plane (blue, Ge; gray, C; red, O). Hydrogen atoms are omitted for clarity. Note that both square-like and rectangular channels attributable to intermolecular hydrogen bonding (red dotted lines) are observed along the [001] direction. (For interpretation of the references to colour in this figure legend, the reader is referred to the web version of this article.)

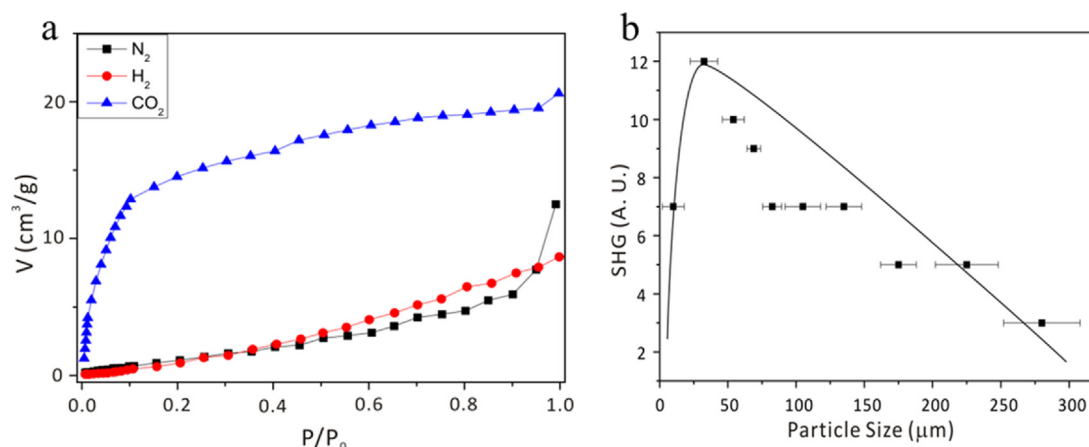


Fig. 3. (a) Adsorption isotherms of N₂ (■, 77 K), H₂ (●, red, 77 K), and CO₂ (▲, blue), 195 K on compound **2**. (b) Phase matching curve (Type 1) for compound **2**. The curve is to guide the eye and is not a fit to the data. (For interpretation of the references to colour in this figure legend, the reader is referred to the web version of this article.)

consistent with that from the crystallographic analysis. The pore size distribution plot has been added to the ESI.

Since compound **2** crystallizes in a noncentrosymmetric space group, its SHG properties were investigated. Powder SHG measurements at 1064 nm radiation indicated that compound **2** has a similar SHG efficiency to that of NH₄H₂PO₄ (ADP), *i.e.*, approximately $10 \times \alpha$ -SiO₂. It is not surprising that the reported material has a relatively weaker SHG efficiency, because no NLO chromophores are found from the central metal cation or ligand in compound **2**. Besides, the material crystallizes in the NCS nonpolar space group, *I*-4. By sieving the polycrystalline sample into various particle sizes, ranging from 20 to 250 μm and measuring the SHG as a function of particle size, the Type 1 phase-matching capability of the material were measured. The powder SHG measurements indicate that compound **2** is not phase-matchable (Fig. 3b), as often reported from the Class C category of SHG materials, as defined by Kurtz and Perry [20].

A novel germanium-organic compound (**2**) possesses two types of distinct channels obtained by intermolecular hydrogen bonding. Thus, the reported compound can be categorized as a porous multifunctional material that is crystallizing in a noncentrosymmetric (NCS) space group with an unprecedented channel structure exhibiting interesting physical properties found from NCS structures.

As a porous molecular material, compound **2** reveals a differential gas adsorption phenomenon and might be used for a gas separation filter. Since the process toward useful devices such as gas separation films and/or filters for porous coordination polymers is much more accessible compared to that of pure inorganic porous materials, the title compound should be very useful for the application. In addition, the reported material shows second-harmonic generations (SHG) properties attributed to the macroscopic asymmetric structure. Therefore, the closely related interesting piezoelectric properties are also expected from the compound. In fact, SHG and piezoelectricity are crucial characteristics for industrial applications such as lasers, optical communications, sensors, actuators, and energy harvesting, etc. It should be pointed that the porous molecular material may reveal all these industrially important properties in one compound.

Compound **2** exhibits a differential gas adsorption property. The Powder SHG measurements indicate that compound **2** has 10 times higher SHG efficiency than those of α -SiO₂ and type-1 nonphase-matchable, indicating that compound **2** might be applied to gas separation and storage by a careful adjustment of the channel size and functionalization of the framework. In addition, the NCS space

group for the compound might be useful for the applications in sensors and energy storage.

Preparation of 2-(4-bromophenyl)-5,5-dimethyl-2-phenyl-1,3-dioxane (**1**)

4-Bromobenzophenone (20.0 g, 76.6 mmol), 2,2-dimethylpropane-1,3-diol (12.0 g, 115.0 mmol), 4-methylbenzenesulfonic acid (0.66 g, 3.84 mmol) was dissolved in toluene (600 ml), and the mixture was heated at reflux for 19 h. The resulting mixture was cooled to room temperature and diluted with CHCl₃. The organic layer was washed with Na₂CO₃ solution, water and brine, dried over anhydrous MgSO₄, filtered, and concentrated in vacuo. The resulting crude product was recrystallized from *iso*-propanol, affording **1** (22.1 g, 83%) as pale pink plate-shaped crystals; TLC $R_f = 0.84$ (*n*-hexane:Et₂O = 2:1); ¹H NMR (600 MHz, CDCl₃) δ 0.97 (s, 3H), 1.02 (s, 3H), 3.61 (q, $J = 11.19$ Hz, 4H), 7.28 (t, $J = 7.35$ Hz, 1H), 7.36 (t, $J = 7.64$ Hz, 2H), 7.41 (d, $J = 8.71$ Hz, 2H), 7.46 (d, $J = 8.67$ Hz, 2H), 7.51 (d, $J = 8.29$ Hz, 2H); ¹³C NMR (150 MHz, CDCl₃) δ 22.49, 22.60, 30.16, 72.08 ($\times 2$), 100.53, 121.92, 126.56 ($\times 2$), 127.98, 128.41 ($\times 2$), 128.49 ($\times 2$), 131.48 ($\times 2$), 141.40, 141.45; GC/MS calcd for C₁₈H₁₉BrO₂ (M⁺): 345.65.

Preparation and crystallization of tetrakis(4-(5,5-dimethyl-2-phenyl-1,3-dioxan-2-yl)phenyl)germane (**2**)

2-(4-Bromophenyl)-5,5-dimethyl-2-phenyl-1,3-dioxane, **1** (15.4 g, 44 mmol) was pre-dried by Ar purging and dissolved in THF (250 mL). To that solution, *n*-BuLi (17.6 mL, 44 mmol, 2.5 M in hexane) was added dropwise under stirring at -78°C in Ar atmosphere. After 30 min of stirring, GeCl₄ (1.00 mL, 8.74 mmol) was added to the solution at -78°C . The reaction mixture was stirred for 3 h at -78°C and 12 h at ambient temperature. The resulting mixture was cooled to room temperature and diluted with CHCl₃. The organic layer was washed with 1% aqueous HCl, water and brine, dried over anhydrous MgSO₄, filtered, and concentrated in vacuo. The resulting crude product was recrystallized from ether, affording **2** (10.4 g, 83%) as colorless plate-shaped single crystals; TLC $R_f = 0.72$ (*n*-hexane:THF = 2:1); ¹H NMR (600 MHz, CDCl₃) δ 0.95 (s, 12H), 1.02 (s, 12H), 3.59 (s, 16H), 7.26 (t, $J = 7.37$ Hz, 4H), 7.34 (t, $J = 7.67$ Hz, 8H), 7.43 (d, $J = 8.41$ Hz, 8H), 7.45 (d, $J = 8.41$ Hz, 8H), 7.50 (d, $J = 8.28$ Hz, 8H); ¹³C NMR (150 MHz, CDCl₃) δ 22.52, 22.63, 30.16, 72.10 ($\times 2$), 100.92, 126.28 ($\times 2$), 126.79 ($\times 2$), 127.78, 128.34 ($\times 2$), 137.37 ($\times 2$), 135.42, 141.56, 142.96; MALDI-TOF MS calcd for C₇₂H₇₆O₈Ge (M⁺): 1143.6421.

Single-crystal X-ray diffraction

The structure of **2** was determined by the standard crystallographic method, using a colorless plate crystal ($0.028 \times 0.034 \times 0.046 \text{ mm}^3$) of **2** for single crystal data analysis. All the data were collected using a Bruker SMART BREEZE diffractometer equipped with a 1 K CCD area detector using graphite monochromated Mo K α radiation at 200 K. A hemisphere of data was collected using a narrow-frame method with the scan widths of 0.30° in omega and an exposure time of 5 s/frame. The first 50 frames were remeasured at the end of the data collection to monitor the instrument and crystal stability. The maximum correction applied to the intensities was $< 1\%$. The data were integrated using the SAINT program, with the intensities corrected for Lorentz factor, polarization, air absorption, and absorption attributable to the variation in the path length through the detector faceplate [21]. The hemisphere of data was corrected using semiempirical absorption with the SADABS program [22]. The data were solved and refined using SHELXS-97 and SHELXL-97, respectively [23,24]. All the atoms except for hydrogen were refined with anisotropic displacement parameters and converged for $I > 2\sigma(I)$. All the calculations were performed using the WinGX-98 crystallographic software package [25]. The crystallographic data and selected bond distances for the reported material are given in Tables 1 and 2 for comparison.

Powder X-ray diffraction

Powder X-ray diffraction was used to confirm the phase purity of the synthesized material. Powder XRD pattern was collected at room temperature using a Bruker D8-Advance diffractometer equipped with Cu K α radiation at 40 kV and 40 mA. The well ground polycrystalline sample of **2** was mounted on a sample

holder and scanned in the 2θ range $5\text{--}70^\circ$ with a step size and step time of 0.02° and 0.2 s, respectively. The experimental powder XRD pattern is in good agreement with the calculated data from the single-crystal model. The XRD patterns can be found in the Electronic Supplementary Information (ESI).

Second-order nonlinear optical measurements

Powder second-harmonic generating (SHG) measurements of polycrystalline material **2** were performed using a modified Kurtz-NLO system using 1064 nm radiation [26]. A DAWA Q-switched Nd:YAG laser, operating at 20 Hz, was used for the measurements. Because the SHG efficiency has been shown to depend strongly on the particle size, polycrystalline samples were ground and sieved (Newark Wire Cloth Co.) into distinct particle size ranges (20–45, 45–63, 63–75, 75–90, 90–125, 125–150, 150–200, 200–250, $> 250 \mu\text{m}$). To make relevant comparisons with the known SHG materials, crystalline $\alpha\text{-SiO}_2$ and LiNbO_3 were also ground and sieved into the same particle size ranges. Powders with the particle size in the range 45–63 μm were used for comparing the SHG intensities. All the powder samples with different particle sizes were placed in separate capillary tubes. No index matching fluid was used in any of the experiments. The SHG light, *i.e.*, 532 nm green light, was collected in reflection and detected using a photomultiplier tube (Hamamatsu). To detect only the SHG light, a 532 nm narrow-pass interference filter was attached to the tube. A digital oscilloscope (Tektronix TDS1032) was used to view the SHG signal. A detailed description of the equipment and the methodology used has been published [27].

Acknowledgments

This research was supported by the Chung-Ang University Graduate Research Scholarship in 2017 and Basic Science Research Program through the National Research Foundation of Korea (NRF) funded by the Ministry of Education [2017R1D1A1B03031915].

Appendix A. Supplementary data

Supplementary data associated with this article can be found, in the online version, at <https://doi.org/10.1016/j.jiec.2018.09.024>.

Table 1
Crystallographic data for **2**.

Empirical formula	GeC ₇₂ H ₇₆ O ₈
Formula weight	1141.94
Crystal system	Tetragonal
Space group	I-4 (No. 82)
$a = b/\text{\AA}$	19.5513(5)
$c/\text{\AA}$	8.3226(3)
$V/\text{\AA}^3$	3181.3(2)
Z	2
$D_c/\text{g cm}^{-3}$	1.192
$R(F)^a$	0.0448
$R_w(F^2)^b$	0.0602
Flack parameter	0.017(12)
Largest residuals/ $e \text{\AA}^{-3}$	0.234 and -0.215

$$^a R(F) = \frac{\sum ||F_o| - |F_c||}{\sum |F_o|}$$

$$^b R_w(F^2) = \left[\frac{\sum w(F_o^2 - F_c^2)^2}{\sum w(F_o^2)^2} \right]^{1/2}$$

Table 2
Selected bond distances (\AA) for **2**.

Ge(1)–C(1) $\times 4$	1.940(3)	C(7)–C(8)	1.533(5)
O(1)–C(7)	1.421(5)	C(8)–C(9)	1.377(5)
O(1)–C(14)	1.441(4)	C(8)–C(13)	1.368(5)
O(2)–C(7)	1.404(4)	C(9)–C(10)	1.397(5)
O(1)–C(15)	1.445(4)	C(10)–C(11)	1.347(8)
C(1)–C(2)	1.371(4)	C(11)–C(12)	1.344(10)
C(1)–C(6)	1.370(4)	C(12)–C(13)	1.407(8)
C(2)–C(3)	1.381(4)	C(14)–C(16)	1.509(5)
C(3)–C(4)	1.371(5)	C(15)–C(16)	1.534(5)
C(4)–C(5)	1.377(4)	C(16)–C(17)	1.525(5)
C(4)–C(7)	1.516(5)	C(16)–C(18)	1.548(5)
C(5)–C(6)	1.380(4)		

References

- [1] J. Kjelstrup-Hansen, J.E. Norton, D.A. Silva Filho, J.L. Bredas, H.G. Rubahn, *Org. Electron.* 10 (2009) 1228.
- [2] S. Kumar, P. Singh, R. Srivastava, S. Ghosh, *RCS Adv.* 5 (2015) 61249.
- [3] A. Cappelli, V. Razzano, G. Fabio, M. Paolini, G. Grisci, G. Giuliani, A. Donati, R. Mendichi, W. Mroz, F. Villafiorita, C. Botta, *RCS Adv.* 5 (2015) 101377.
- [4] Y.J. Shirota, *Mater. Chem.* 15 (2005) 75.
- [5] S. Wang, W.J. Oldham, R.A. Hudack, G.C. Bazan, *J. Am. Chem. Soc.* 122 (2000) 5695.
- [6] S.-K. Kim, Y.-I. Park, I.-N. Kang, J.-W. Park, *J. Mater. Chem.* 17 (2007) 4670.
- [7] S. Liu, F. He, H. Wang, H. Xu, C. Wang, F. Li, Y. Ma, *J. Mater. Chem.* 18 (2008) 4802.
- [8] S.-C. Lo, P.L. Burn, *Chem. Rev.* 107 (2007) 1097.
- [9] P. Furuta, J. Brooks, M.E. Thompson, J.M.J. Fréchet, *J. Am. Chem. Soc.* 125 (2003) 13165.
- [10] Y.-Y. Lyu, J. Kwak, W.S. Jeon, Y. Byun, H.S. Lee, D. Kim, C. Lee, K. Char, *Adv. Funct. Mater.* 19 (2009) 420.
- [11] C.M. Kim, M.J. Yoon, S.H. Hong, K.Y. Park, S.Y. Kim, *Electron. Mater. Lett.* 12 (2016) 388.
- [12] A.L. Spek, Platon, A Multi-Purpose Crystallographic Tool, Utrecht University, Utrecht, The Netherlands, 2001.
- [13] D.N. Dybtsev, H. Chun, S.H. Yoon, D. Kim, K. Kim, *J. Am. Chem. Soc.* 126 (2004) 32.
- [14] T.K. Maji, R. Matsuda, S. Kitagawa, *Nat. Mater.* 6 (2007) 142.
- [15] K.M. Ok, J. Sung, G. Hu, R.M.J. Jacobs, D. O'Hare, *J. Am. Chem. Soc.* 130 (2008) 3762.
- [16] H.J. Lee, W. Cho, S. Jung, M. Oh, *Adv. Mater.* 21 (2009) 674.
- [17] P.S. Nugent, V.L. Rhodus, T. Pham, K. Forrest, L. Wojtas, B. Space, M.J. Zaworotko, *J. Am. Chem. Soc.* 135 (2013) 10950.

- [18] N.H. Lee, D.W. Lee, H. Yeo, K. Kwak, H.S. Chun, K.M. Ok, *CrystEngComm* 16 (2014) 5619.
- [19] W. Steele, *Chem. Rev.* 93 (1993) 2355.
- [20] S.K. Kurtz, T.T. Perry, *J. Appl. Phys.* 39 (1968) 3798.
- [21] SAINT, Program for Area Detector Absorption Correction, version 4.05, Siemens Analytical X-ray Instruments, Madison, WI, USA, 1995.
- [22] R.H. Blessing, *Acta Crystallogr. A* 51 (1995) 33.
- [23] G.M. Sheldrick, SHELXS-97, A Program for Automatic Solution of Crystal Structures, University of Goettingen, Goettingen, Germany, 1997.
- [24] G.M. Sheldrick, SHELXL-97, A Program for Crystal Structure Refinement, University of Goettingen, Goettingen, Germany, 1997.
- [25] L.J. Farrugia, *J. Appl. Crystallogr.* 32 (1999) 837.
- [26] S.K. Kurtz, T.T. Perry, *J. Appl. Phys.* 39 (1968) 3798.
- [27] K.M. Ok, E.O. Chi, P.S. Halasyamani, *Chem. Soc. Rev.* 35 (2006) 710.